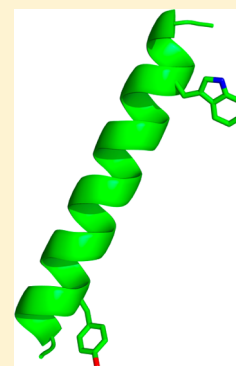


Tyrosine Replacing Tryptophan as an Anchor in GWALP Peptides

Nicholas J. Gleason,[†] Vitaly V. Vostrikov,[†] Denise V. Greathouse,[†] Christopher V. Grant,[‡] Stanley J. Opella,[‡] and Roger E. Koeppe, II^{*,†}[†]Department of Chemistry and Biochemistry, University of Arkansas, Fayetteville, Arkansas 72701, United States[‡]Department of Chemistry and Biochemistry, University of California, San Diego, La Jolla, California 92093, United States

S Supporting Information

ABSTRACT: Synthetic model peptides have proven useful for examining fundamental peptide–lipid interactions. A frequently employed peptide design consists of a hydrophobic core of Leu-Ala residues with polar or aromatic amino acids flanking each side at the interfacial positions, which serve to “anchor” a specific transmembrane orientation. For example, WALP family peptides (acetyl-GWW(LA)_nLWWA-[ethanol]amide), anchored by four Trp residues, have received particular attention in both experimental and theoretical studies. A recent modification proved successful in reducing the number of Trp anchors to only one near each end of the peptide. The resulting GWALP23 (acetyl-GGALW^S(LA)₆LW¹⁹LAGA-[ethanol]amide) displays reduced dynamics and greater sensitivity to lipid–peptide hydrophobic mismatch than traditional WALP peptides. We have further modified GWALP23 to incorporate a single tyrosine, replacing W^S with Y^S. The resulting peptide, Y^SGWALP23 (acetyl-GGALY^S(LA)₆LW¹⁹LAGA-amide), has a single Trp residue that is sensitive to fluorescence experiments. By incorporating specific ²H and ¹⁵N labels in the core sequence of Y^SGWALP23, we were able to use solid-state NMR spectroscopy to examine the peptide orientation in hydrated lipid bilayer membranes. The peptide orients well in membranes and gives well-defined ²H quadrupolar splittings and ¹⁵N/¹H dipolar couplings throughout the core helical sequence between the aromatic residues. The substitution of Y^S for W^S has remarkably little influence on the tilt or dynamics of GWALP23 in bilayer membranes of the phospholipids DOPC, DMPC, or DLPC. A second analogue of the peptide with one Trp and two Tyr anchors, Y^{4,5}GWALP23, is generally less responsive to the bilayer thickness and exhibits lower apparent tilt angles with evidence of more extensive dynamics. In general, the peptide behavior with multiple Tyr anchors appears to be quite similar to the situation when multiple Trp anchors are present, as in the original WALP series of model peptides.



Because characterizing the structures and functional properties of membrane proteins is generally a more complicated task than for aqueous soluble proteins, synthetic model membrane peptides have proven to be valuable for discerning fundamental principles that govern protein–lipid interactions. These chemically well-defined peptide systems offer opportunities for examining direct lipid interactions by placing limits upon external factors such as multiple transmembrane helices, large steric effects, or interactions in oligomers. One of the first such peptide sequences was KK(L)₂₄KKA-amide.^{1,2} This sequence was chosen because it consists of a hydrophobic polyleucine α -helix that was expected to associate with the acyl chains in a lipid bilayer membrane flanked on the ends by two hydrophilic, charged lysine residues that are expected to be soluble in the aqueous environment adjacent to the membrane. In model membrane-spanning peptides, the N- and C-termini generally are capped to render them uncharged. Later peptide models incorporated an interior helical (Leu-Ala)_n core sequence, which resulted in a lower overall hydrophobicity and an increased sensitivity to the identities of the lipids that compose the bilayer.³

A survey of type I single-span membrane proteins revealed a nonrandom distribution of the aromatic Trp, Tyr, and Phe residues.⁴ These aromatic residues are typically located near the aqueous–lipid interface where they are believed to act as

anchors to help position the transmembrane helix within the bilayer.⁵ Other experiments with gramicidin A revealed that the Trp preference for the membrane interfacial region promotes lipid H_{II} phase formation⁶ as well as assembly of dimeric gramicidin channels in lipid bilayer membranes.⁷ WALP peptides (acetyl-GWW(LA)_nLWWA-[ethanol]amide) incorporating multiple Trp anchors and the helical, hydrophobic repeating Leu-Ala core sequence induced lipid phase changes, similar to gramicidin A, as a function of lipid–peptide hydrophobic mismatch.⁸ Later the four Trp anchor residues were mutated to various other aromatic or charged residues (Tyr, Phe, Lys, Arg, or His) to monitor the importance of the anchor's chemical and physical properties.^{9,10} These model peptides helped to describe the properties, such as peptide-dependent lipid phase behavior and lipid ordering, caused by the hydrophobic mismatch. In 2002, it was reported that WALP peptides have a characteristic nonzero tilt with respect to a lipid bilayer normal;¹¹ on theoretical grounds the fundamental tilt subsequently was attributed to the entropy of precession about the bilayer normal.¹² The ability to decrease the number of

Received: November 21, 2011

Revised: February 24, 2012

Published: February 24, 2012

anchor residues has been demonstrated with (acetyl-GGALW-(LA)₆LWLAGA-[ethanol]amide), which possesses only one Trp anchor near each of the termini.¹³ The tryptophans in GWALP23 flank a hydrophobic Leu-Ala core of the same length as that of WALP19.^{8,11} With fewer anchor residues, it becomes easier to assess the roles of each of them. For example, the measured ²H quadrupolar splittings and apparent tilt angle of GWALP23 in lipid bilayers are much more responsive than those of WALP19 or WALP23 to the lipid hydrophobic thickness.¹⁴ Furthermore, the average tilt direction of GWALP23 remains essentially constant in lipid bilayers of different thickness.¹⁴ These results suggest that the four Trp anchors in the original WALP series of peptides are so dominating that they induce significant peptide dynamics, and variations in the tilt direction,¹⁴ while resisting significant changes to the magnitude of the apparent average tilt angle, even in cases where the bilayer thickness changes.

A further step beyond GWALP23 would be to replace one of the two remaining tryptophans with another chemically different anchoring residue. An advantage of such an approach would be to open a window for fluorescence experiments involving the single remaining Trp residue. To this end, we have investigated the influence of a single Trp to Tyr replacement upon GWALP23. The choice of tyrosine is based upon our preference to retain an aromatic residue and an uncharged “host” peptide (in preparation for future experiments that could investigate the introduction of a variety of “guest” charged residues within a parent peptide). We have synthesized a new peptide Y⁵GW¹⁹ALP23 (acetyl-GGALY-(LA)₆LWLAGA-amide) and have incorporated deuterated alanine residues and ¹⁵N-labeled residues in selected sequence positions for analysis by solid-state NMR. Using circular dichroism spectroscopy, solid-state ²H NMR spectroscopy with “geometric analysis of labeled alanines” (GALA),¹¹ and solid-state ¹⁵N/¹H high-resolution separated local field NMR spectroscopy,^{15,16} we have characterized the properties of Y⁵GW¹⁹ALP23 in lipid bilayer membranes of DOPC, DMPC, and DLPC. Additionally, we incorporated a second tyrosine to form Y^{4,5}GW¹⁹ALP23 and compared the orientation and dynamics of the “double-tyrosine” anchored peptide with those of Y⁵GW¹⁹ALP23 in the three different lipid bilayer membranes.

Knowledge of the orientations and dynamics of model transmembrane helices is significant for understanding principles that undergird not only the structure and function of membrane proteins in general but also the mechanisms of signaling.^{17,18} To this end, it is important to have robust model systems that will establish a vigorous framework for such understanding.

MATERIALS AND METHODS

Solid Phase Synthesis of ²H-Labeled Peptides.

Commercial L-alanine-*d*₄ from Cambridge Isotope Laboratories (Andover, MA) was modified with an Fmoc group, as described previously,¹⁹ and recrystallized from ethyl acetate:hexane, 80:20. NMR spectra (¹H) were used to confirm successful Fmoc-Ala-*d*₄ synthesis. Fmoc-L-Ala-¹⁵N and Fmoc-L-Leu-¹⁵N were purchased from Cambridge. Other protected amino acids and acid-labile “Rink” amide resin were purchased from NovaBiochem (San Diego, CA). All peptides were synthesized on a 0.1 mmol scale using “FastMoc” methods and a model 433A synthesizer from Applied Biosystems by Life Technologies (Foster City, CA). Typically, two deuterated alanines of

differing isotope abundances were incorporated into each synthesized peptide. Selected precursors for deuterated residues therefore contained either 100% Fmoc-L-Ala-*d*₄ or 60% Fmoc-L-Ala-*d*₄ with 40% nondeuterated Fmoc-L-Ala. Some peptides were synthesized without deuterium, but with 100% abundance of ¹⁵N in selected residues. The final residue on each peptide was acetyl-Gly to yield a blocked, neutral N-terminal.

A peptide cleavage solution was prepared containing 85% trifluoroacetic acid (TFA) and 5% each (v/v or w/v) of triisopropylsilane, water, and phenol. TFA cleavage from “Rink” resin in 2 mL volume (2–3 h at 22 °C) leads to a neutral, amidated C-terminal. Peptides were precipitated by adding the TFA solution to 25 volumes of cold 50/50 MtBE/hexane. Peptides were collected by centrifugation, washed multiple times with MtBE/hexane, and lyophilized multiple times from (1:1) acetonitrile/water to remove residual TFA. MALDI-TOF mass spectrometry was used to confirm peptide molecular mass (Figure S1 in Supporting Information). Peptide purity was examined by reversed-phase HPLC with 280 nm detection, using a 4.6 × 50 mm Zorbax SB-C8 column packed with 3.5 μm octyl-silica (Agilent Technologies, Santa Clara, CA), operated at 1 mL/min using a methanol/water gradient from 85% to 99% methanol (with 0.1% TFA) over 5 min (Figure S2 in Supporting Information). Peptide amounts were measured by means of UV absorbance at 280 nm, using molar extinction coefficients of 5600 M⁻¹ cm⁻¹ for each Trp and 1490 M⁻¹ cm⁻¹ for each Tyr residue in the peptide.²⁰ Solvents were of the highest available purity. Water was doubly deionized Milli-Q water.

²H NMR Spectroscopy Using Oriented Bilayer Samples. Mechanically aligned samples for solid-state NMR spectroscopy (1/60, peptide/lipid) were prepared using DOPC, DMPC, or DLPC lipids from Avanti Polar Lipids (Alabaster, AL) and deuterium-depleted water (Cambridge; 45% w/w hydration), as described previously.¹¹ Bilayer alignment within each sample was confirmed using ³¹P NMR at 50 °C on a Bruker Avance 300 spectrometer (Billerica, MA) at both β = 0° (bilayer normal parallel to magnetic field) and β = 90° macroscopic sample orientations (Figure S3 in Supporting Information). Deuterium NMR spectra were recorded at 50 °C using both sample orientations on a Bruker Avance 300 spectrometer, utilizing a quadrupolar echo pulse sequence²¹ with 90 ms recycle delay, 3.2 μs pulse length, and 115 μs echo delay. Between 0.6 and 1.5 million scans were accumulated during each ²H NMR experiment. An exponential weighting function with 100 Hz line broadening was applied prior to Fourier transformation.

¹⁵N NMR Spectroscopy Using Magnetically Oriented Bicelles. Magnetically oriented bicelles for solid-state ¹⁵N NMR spectroscopy (1/80, peptide/total lipid) were prepared using DMPC-ether and DHPC-ether lipids (3.2/1.0, mol/mol; *q* value) from Avanti Polar Lipids (Alabaster, AL), in a total volume of 175 μL of deuterium-depleted water (Cambridge). Peptide and DHPC-ether were mixed and then dried under nitrogen flow and vacuum to remove organic solvent. Separate samples of the DMPC-ether lipid also were prepared in aliquots and dried. Peptide/DHPC-ether films were hydrated using 100 μL of water and DMPC-ether with 75 μL of water. After the contents of two separate vials were dissolved, the peptide/DHPC-ether solution was transferred to the DMPC-ether solution. Contents were cycled between 0 and 45 °C several times, with intermittent vortexing, until the solution remained

clear when cold. While still cold, the bicelle sample solution was transferred to a 5 mm NMR tube and sealed.

For ^{15}N -based SAMPI4 experiments (in the same family of pulse sequences as PISEMA), GWALP23 and $\text{Y}^5\text{GWALP23}$ enriched in ^{15}N leucine and alanine were synthesized (five labels, residues 13–17). ^{15}N chemical shifts and $^{15}\text{N}/^1\text{H}$ dipolar coupling values were recorded using 500 MHz Bruker Avance and Varian Inova spectrometers and established pulse sequences.^{15,22–24} Solid-state NMR high-resolution separated local field SAMPI4 experiments²⁵ were performed using a 1 ms CP contact time and rf field strengths of ~ 50 kHz; 54 t1 points were acquired using 8.0 ms of acquisition time in the direct (t2) dimension and a 7.5 s recycle delay. The sample temperature was maintained at 42 °C, just below a critical temperature for structural transformation of DMPC/DHPC bicelle samples.²⁶ We have found that the peptide order parameter is essentially unchanged between DMPC/DHPC bicelles at 42 °C and bilayer plate samples at 50 °C,²⁷ where the spectral quality often improves for the plate samples.²⁸ Attempts were made also to construct DLPC-based “bicelles” using DLPC-ether, DHPC-ether, and dipentanoyl-PC (13.3/3/1) with peptide incorporated at 1/80 (peptide/DLPC; mol/mol).²⁹ Unfortunately, initial efforts did not yield well-oriented bicelles; thus, we were unable to resolve the $^{15}\text{N}/^1\text{H}$ dipolar couplings or assign the ^{15}N chemical shift frequencies for such samples using the ^{15}N -based SAMPI4 experiments.

Data Analysis. Combinations of ^2H quadrupolar splittings and $^{15}\text{N}/^1\text{H}$ dipolar coupling frequencies, individually or together, and in some cases along with ^{15}N chemical shift values, were used to calculate the orientations of the peptide helix in the bilayers. Data uncertainty was estimated to be within ± 0.5 kHz based on duplicate samples and measurements using different orientations of glass slide samples.²⁷ We performed calculations both with a semistatic (variable S_{zz}) model³⁰ and with a more dynamic model that incorporates Gaussian distributions for the tilt and direction of tilt.³⁰ The detailed strategy for combined ^2H and $^{15}\text{N}/^1\text{H}$ analysis has been described.²⁷

The analysis using semistatic peptide dynamics involves a principal order parameter S_{zz} to estimate overall peptide motion with respect to an apparent average peptide orientation. These calculations are based on the GALA analysis, as previously described.^{11,30,31} For samples in DMPC, we incorporate also $^{15}\text{N}/^1\text{H}$ dipolar coupling and ^{15}N chemical shift values obtained from SAMPI4 spectra to determine a best fit to the experimental data.³² These calculations are performed using helix tilt τ , rotation ρ about the helix axis, and a principal order parameter S_{zz} as variable parameters. The analysis takes into account the ^2H quadrupolar splittings and/or $^{15}\text{N}/^1\text{H}$ dipolar coupling frequencies and ^{15}N chemical shifts for the isotope-labeled residues based on ideal α -helix geometry.

To proceed beyond a semistatic model, we performed calculations that take into account more complex peptide dynamics, in which σ_τ and σ_ρ relate to the widths of Gaussian distributions for the peptide tilt and rotation.³⁰ In this analysis, a principal order parameter S_{zz} is fixed at 0.88 to reflect isotropic fluctuations, and further anisotropic variations in τ and ρ are permitted. A best-fit rmsd to observed dipolar and quadrupolar couplings, and ^{15}N chemical shift values, is based upon the parameters τ_0 , ρ_0 , σ_τ , and σ_ρ , following ref 30. Fixed parameters in the analysis included chemical shift tensor components (σ_{11} , σ_{22} , σ_{33}) of (64, 77, 224) ppm, as reported for model dipeptides³³ and small proteins,³⁴ a coupling constant of

10.22 kHz (based on an NH bond length of 1.06 Å),^{35,36} and the angle ε_{\parallel} (14°) between the peptide helix axis and the N–H bond. In the combined analysis, equal weights were assigned to the ^2H methyl quadrupolar couplings, $^{15}\text{N}/^1\text{H}$ dipolar coupling frequencies, and the ^{15}N chemical shift frequencies. Further details are described in refs 27 and 37.

CD Spectroscopy. Small lipid vesicles incorporating 125 nM peptide and 7.5 μM lipid (1/60) were prepared by sonication in unbuffered water. An average of 10 scans was recorded on a Jasco (Easton, MD) J710 CD spectropolarimeter, using a 1 mm cell path length, 1.0 nm bandwidth, 0.1 nm slit, and a scan speed of 20 nm/min.

Steady-State Fluorescence Spectroscopy. Vesicle solutions with 1/60 peptide/lipid for fluorescence experiments were prepared by dilution, 1/20 with water, of the samples prepared previously for CD spectroscopy (above). Samples were excited at 280 or 295 nm with a 5 nm excitation slit, and emission spectra were recorded between 300 and 420 nm with a 5 nm emission slit using a Hitachi F-2500 fluorescence spectrophotometer. The spectra from five scans were averaged.

RESULTS

Synthetic WALP peptides as well as analogues such as GWALP23 possess primarily α -helical character that is typical of transmembrane segments and is expected from the repeating Leu-Ala core residues, which possess a propensity for forming helices. When the L^4W^5 sequence of GWALP23 is replaced

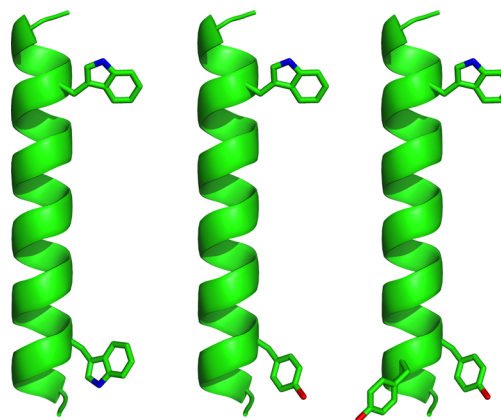


Figure 1. Representative models of GWALP23, $\text{Y}^5\text{GWALP23}$, and $\text{Y}^{4,5}\text{GWALP23}$ (left to right), showing the locations of aromatic side chains on a ribbon helix, drawn using PyMOL.⁴⁶ The side-chain orientations are arbitrary.

with L^4Y^5 or Y^4Y^5 , the resulting peptides have “single” or “double” Tyr anchors N-terminal to the core $(\text{Leu-Ala})_n$ sequence. Circular dichroism spectra for such peptides in lipid bilayer membranes demonstrate equal or slightly reduced α -helical character when the Tyr anchor(s) are present, compared to GWALP23 (Figure 2). In particular, the presence of Y^4 as a second “anchor” residue seems to have little influence on the CD spectrum or the magnitudes of the peaks that characterize α -helices. Importantly, both the Y^5 and $\text{Y}^{4,5}$ derivatives maintain primarily an α -helical backbone structure. With sample formulation being vesicles for the CD spectra, stacked bilayers for the ^2H NMR spectra, and bicelles for the $^{15}\text{N}/^1\text{H}$ NMR spectra, we believe that the core domains of the peptides are helical in all of the lipid membrane environments. Indeed, the ^2H resonances show agreement between bicelles

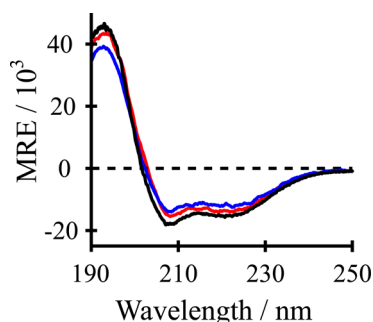


Figure 2. Circular dichroism spectra of GWALP23 (black), Y⁵GWALP23 (blue), and Y^{4,5}GWALP23 (red) in DLPC vesicles.

and bilayers²⁷ and follow a helical pattern for the core alanines, while also illustrating helix unwinding in the vicinity of A³ and A²¹, outside of the central core sequence.¹⁴

Further information was obtained from oriented lipid bilayer samples that included the ²H-labeled Tyr-containing peptides at a peptide:lipid molar ratio of 1:60. For such samples, ³¹P NMR spectra confirmed that the bilayers were well aligned with respect to the magnetic field (Supporting Information, Figure S3). For the $\beta = 90^\circ$ sample orientation, a strong single ³¹P resonance was observed at ~ -24 ppm (with the precise chemical shift frequency varying from -22.4 to -26.3 ppm in the DLPC, DMPC, and DOPC lipid bilayer membranes). When samples were oriented at $\beta = 0^\circ$, a strong peak at $\sim +18$ ppm was observed as well as small amounts of unoriented lipids that comprised a minor peak around -24 ppm.

The ²H NMR spectra display the two expected pairs of resonances corresponding to the quadrupolar splittings from the two labeled Ala methyl side chains in each peptide. Figure 3

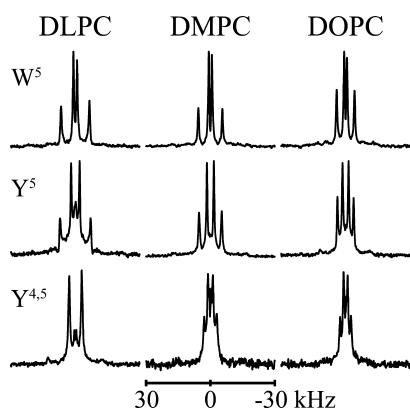


Figure 3. ²H NMR spectra of (top to bottom) GWALP23, Y⁵GWALP23, and Y^{4,5}GWALP23, each labeled at Ala¹⁷ (100% ²H) and Ala⁷ (60% ²H), in hydrated oriented bilayers of DLPC, DMPC, and DOPC. Peptide/lipid ratio, 1/60 (mol/mol); 50 °C; $\beta = 90^\circ$ sample orientation.

includes the spectra for alanines 7 and 17 in GWALP23, Y⁵GWALP23, and Y^{4,5}GWALP23, each incorporated in DLPC, DMPC, and DOPC bilayer membranes. The spectra for the other labeled alanines are included as Supporting Information (Figures S4 and S5). In rare cases, single sets of broad peaks were observed due to spectral overlap arising from similar ²H quadrupolar splittings from the two alanines. When the plate samples are turned from the $\beta = 0^\circ$ orientation to $\beta = 90^\circ$, the quadrupolar splittings are found to be reduced by a factor of 2. The appearance of sharp resonances with half-magnitude

quadrupolar splittings at $\beta = 90^\circ$ illustrates that the peptides undergo fast axial rotational diffusion about the bilayer normal on the NMR time scale.³⁸ It should be noted that the fast rotational averaging about the precession axis (bilayer normal) is distinct from averaging about the helix axis which, if complete, could average all of the ²H Ala signals to a common value,¹¹ contrary to what is observed.

Table 1. Sequences of GWALP23 and Related Peptides^a

name	sequence
WALP23	a-GWW ³ LALALALALALALWWA-e
WALP19	a-GWW ³ LALALALALALALWWA-e
GWALP23	a-GGALW ⁵ LALALALALALALWLAGA-e
Y ⁵ GWALP23	a-GGALY ⁵ LALALALALALALWLAGA-amide
Y ^{4,5} GWALP23	a-GGAYY ⁵ LALALALALALALWLAGA-amide

^aAbbreviations: “a” denotes “acetyl” and “e” denotes “ethanolamide”.

Y⁵GWALP23 produced a relatively large range of ²H quadrupolar splitting magnitudes, from 8 kHz up to 30 kHz in DLPC (Table 2), suggesting a significant tilt of the peptide helix with respect to the bilayer normal. Somewhat smaller ranges of 4–23 and 1–17 kHz were observed for Y⁵GWALP23 in DMPC and DOPC, respectively. It is also noteworthy that the quadrupolar splittings for Y⁵GWALP23 are in each case within 0.1–4 kHz of the corresponding Ala CD₃ signals in GWALP23,¹⁴ suggesting that the Y⁵ and W⁵ peptides may adopt similar membrane orientations.

In contrast, the double-anchored Y^{4,5}GWALP23 exhibits a much smaller range of quadrupolar splittings, varying only between 1 and 12 kHz in all three lipid bilayers (Table 2). The signals from Y^{4,5}GWALP23 do not appear to be similar to those from GWALP23 or Y⁵GWALP23 in any of the lipid systems. Additionally, the range of quadrupolar splitting frequencies for Y^{4,5}GWALP23 remains approximately the same in each type of lipid bilayer membrane, regardless of the bilayer thickness. The quadrupolar splitting magnitudes for each of the six core alanine methyl side chains in Y⁵GWALP23 and Y^{4,5}GWALP23 are listed in Table 2 for each of the DLPC, DMPC, and DOPC bilayer membrane environments.

Additional orientation information was derived from ¹⁵N-based SAMPI4 experiments that utilized magnetically aligned peptide-containing bicelles composed of the ether analogues of DMPC and DHPC ($q = 3.2:1$, mol:mol). In these experiments, similar ranges are observed for the ¹⁵N chemical shift frequencies of residues 13–17 in GWALP23 (85–100.7 ppm) and Y⁵GWALP23 (84–101 ppm; see Table 3). While the corresponding ¹⁵N/¹H dipolar coupling frequencies also are very similar, the ones for Y⁵GWALP23 are slightly yet systematically smaller in magnitude (0.2–0.5 kHz) than those for GWALP23, resulting in a SAMPI4 spectrum that appears to be somewhat below that of GWALP23 (Figure 4).

Tilt Magnitude, Direction, and Dynamics of Y⁵GWALP23. For Y⁵GWALP23 in DMPC, we utilized a combined analysis of available data from ²H and ¹⁵N solid-state NMR experiments,^{27,37} using Gaussian as well as semistatic treatments of the dynamics. For the DMPC environment, we have a large collection of six ²H-Ala methyl quadrupolar splitting magnitudes, together with the ¹⁵N chemical shift frequencies and ¹⁵N/¹H dipolar coupling frequencies from residues 13–17 (Figures 3 and 4; Tables 2 and 3), giving a total of 16 restraints. For the DLPC environment, we calculated Gaussian and semistatic fits to the dynamics using the six ²H-

Table 2. Observed Ala Methyl ^2H Quadrupolar Splittings^a for GWALP23^b and Tyr-Based Analogues in Three Lipids

residue	DLPC			DMPC			DOPC		
	W ^{5,19}	Y ⁵ W ¹⁹	Y ^{4,5} W ¹⁹	W ^{5,19}	Y ⁵ W ¹⁹	Y ^{4,5} W ¹⁹	W ^{5,19}	Y ⁵ W ¹⁹	Y ^{4,5} W ¹⁹
7	26.4	29.3	11.6	21.9	22.8	11.7	16.6	16.2	10.2
9	25.5	24.0	0.5	8.9	9.2	3.2	1.7	0.5	3.8
11	26.9	26.4	6.9	20.9	20.3	10.7	16.7	13.6	10.0
13	14.6	10.5	4.6	3.8	3.9	2.8	1.5	0.5	3.8
15	20.7	19.5	6.9	17.6	15.6	10.7	15.4	13.6	12.6
17	3.4	8.1	11.6	2.9	5.6	4.4	2.6	4.8	3.8

^aQuadrupolar splittings are reported in kHz for the $\beta = 0^\circ$ sample orientation of GWALP23 (having W5 and W19), Y⁵GWALP23, and Y^{4,5}GWALP23. Each value is an average of (the magnitude observed when $\beta = 0^\circ$) and (twice the magnitude observed when $\beta = 90^\circ$). ^bValues for GWALP23 from ref 14. The positions of the aromatic residues in the peptides are listed as W^{5,19}, Y⁵W¹⁹, and Y^{4,5}W¹⁹.

Table 3. Dipolar Couplings and ^{15}N Chemical Shift Values for Peptide $^{15}\text{N}/^1\text{H}$ Groups^a

residue	GWALP23		Y ⁵ GWALP23	
	^{15}N , ppm	$^{15}\text{N}/^1\text{H}$, kHz	^{15}N , ppm	$^{15}\text{N}/^1\text{H}$, kHz
13	101	3.0	101	2.8
14	87	2.4	88	2.0
15	85	3.4	84	2.9
16	94	3.8	93	3.4
17	97	2.8	99	2.5

^aValues were measured in DMPC/DHPC bicelles and correspond to a $\beta = 90^\circ$ sample orientation.

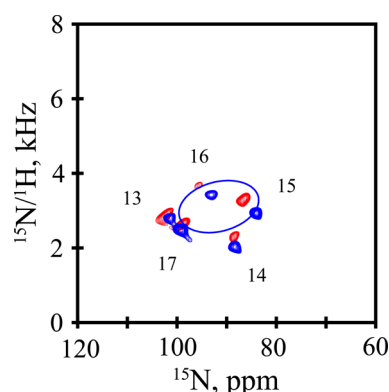


Figure 4. SAMPI4 spectra, with assignments, for GWALP23 (red) and Y⁵GWALP23 (blue, with PISA wheel corresponding to the combined fit to ^{15}N and ^2H data, Table 4), each ^{15}N labeled in residues 13–17. Peptide/lipid ratio, 1/80 (mol/mol); 42 °C; bicelles of DMPC/DHPC ($q = 3.2$).

Ala methyl quadrupolar splittings from macroscopically oriented DLPC bilayers (Table 2; Figure 3).

The fits from the combined analysis of the ^2H and $^{15}\text{N}/^1\text{H}$ NMR data are quite good, with only minor discrepancies between the independent data sets (Figure 5; see Discussion). Importantly, the overall rmsd values of about 1.2 kHz (Table 4) from the combined fits are consistent with the uncertainty of the experimental measurements and suggest no overfitting of the data. The quadrupolar and dipolar wave plots (Figure 5A,B) appear similar for the Gaussian and semistatic analysis methods, with data points close to the analytical curves that result from the combined analysis. Taken together, the independent measurements and the overall agreement lend confidence to the deduced molecular orientations and dynamics for the transmembrane peptides. The influence of the dynamics is evident from the $\sim 10^\circ$ smaller best-fit τ_0 for the semistatic as

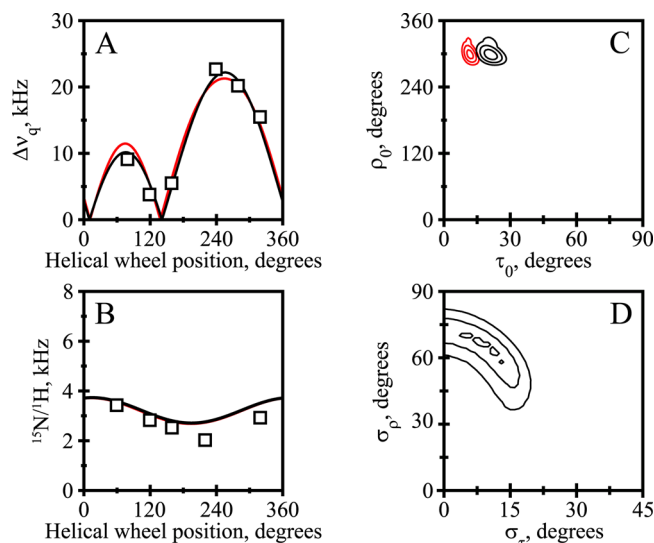


Figure 5. Combined ^{15}N and ^2H analysis for Y⁵GWALP23 in DMPC. (A) Quadrupolar waves from Gaussian dynamics (black curve) and semistatic (red curve) analysis. (B) Dipolar waves from Gaussian (black curve) and semistatic (red curve) analysis. (C) The rmsd (τ_0 , ρ_0) graph for the Gaussian (black contours) and semistatic (red contours) analyses, contoured at 1.5, 2.0, and 2.5 kHz. (D) The rmsd (σ_r , σ_p) graph for the Gaussian dynamics analysis, contoured at 0.95, 1.15, and 1.35 kHz.

opposed to the Gaussian analysis (Figure 5C). As has been characterized for other derivatives of GWALP23,²⁷ four closely spaced minima are observed for the best-fit values of (σ_r , σ_p) (Figure 5D), with each minimum giving similar estimates for τ_0 and ρ_0 .

The dynamics as well as the average orientation of Y⁵GWALP23 and GWALP23 are very similar in DMPC bilayers, regardless of whether Gaussian or semistatic approximations are employed to represent the peptide dynamics (Table 4). In DMPC, the Y5 and W5 peptides show similar small σ_r values (5° – 10°) and similar moderate to large σ_p values (65° – 70°). The apparent tilt angles for the two peptides in DMPC also are nearly identical; namely, τ_0 for both the Y5 and W5 peptides is about 21° based on the Gaussian analysis or about 10° smaller (“apparent” tilt magnitude) when using the semistatic analysis (which ignores σ_p ; Table 4). Again comparing anchor residue Y5 to W5, the direction of peptide tilt ρ_0 differs consistently by about 10° (Table 4), regardless of the method of analysis or whether the host lipid bilayer is DMPC or DLPC.

Table 4. Calculated Orientations and Dynamics of Peptides in DMPC and DLPC^a

peptide	lipid	model	τ_0 (deg)	σ_τ (deg)	ρ_0 (deg)	σ_ρ (deg)	S_{zz}	rmsd (kHz)	n^b
GWALP23	DMPC	Gaussian	21	5	306	70	0.88 ^c	1.1	16
	DMPC	semistatic	11	n.a. ^d	307	n.a. ^d	0.75	1.2	16
Y ⁵ GWALP23	DMPC	Gaussian	21	9	298	66	0.88 ^c	1.2	16
	DMPC	semistatic	12	n.a. ^d	298	n.a. ^d	0.73	1.2	16
GWALP23	DLPC	Gaussian	23	15	304	33	0.88 ^c	0.7	6
	DLPC	semistatic	21	n.a. ^d	305	n.a. ^d	0.71	0.7	6
Y ⁵ GWALP23	DLPC	Gaussian	21	12	295	27	0.88 ^c	0.7	6
	DLPC	semistatic	19	n.a. ^d	295	n.a. ^d	0.78	0.7	6
Y ^{4,5} GWALP23	DLPC	Gaussian	11	27	261	60	0.88 ^c	1.5	6
	DLPC	semistatic	5	n.a. ^d	260	n.a. ^d	0.66	1.6	6

^aThe Gaussian model for the dynamics uses a fixed principal order parameter S_{zz} ³⁰ representing the dynamic extent of (mis)alignment (angle α) between the molecular z-axis and its average orientation, characterized by the time average $S_{zz} = \langle 3 \cos^2 \alpha - 1 \rangle / 2$.⁴⁷ Within this context, further motions can be characterized by the widths σ_τ and σ_ρ of Gaussian distributions about the average values of tilt magnitude τ_0 and tilt direction ρ_0 .³⁰ An alternative semistatic analysis, using three parameters instead of four, determines the best fit (lowest rmsd, in kHz) as a function of τ_0 , ρ_0 , and a variable S_{zz} . ^bNumber of data points (from Tables 2 and 3), identified as six ²H methyl quadrupolar couplings, either alone or with five ¹⁵N/¹H dipolar couplings and ¹⁵N chemical shifts. ^cFixed value. ^dNot applicable.

Table 5. Semistatic GALA Analysis of GWALP23 and Tyr-Anchored Analogues^a

aromatic residues	DLPC				DMPC				DOPC			
	τ_0 (deg)	ρ_0 (deg)	S_{zz}	rmsd (kHz)	τ_0 (deg)	ρ_0 (deg)	S_{zz}	rmsd (kHz)	τ_0 (deg)	ρ_0 (deg)	S_{zz}	rmsd (kHz)
W ^{5,19} ^b	21	305	0.71	0.7	9	311	0.88	1.0	6	323	0.87	0.6
Y ⁵ W ¹⁹	19	295	0.78	0.7	10	300	0.84	0.7	5	311	0.84	1.0
Y ^{4,5} W ¹⁹	5	260	0.66	1.6	3	323	0.77	0.6	3	359	0.82	1.1

^aCalculations based on six Ala methyl ²H quadrupolar splittings only. The reduced S_{zz} values, variable apparent ρ_0 values, and low apparent τ_0 values render Y^{4,5}GWALP23 the outlier among this set of peptides. ^bValues for GWALP23 from ref 14.

In DLPC, the dynamics and average orientation of Y⁵GWALP23 and GWALP23 are also very similar (Table 4). In these cases the Gaussian and semistatic fits to the dynamics, based on six ²H quadrupolar splittings for each, yield similar τ_0 values (about 21°). The Gaussian parameters in DLPC are modest, about 15° for σ_τ and about 30° for σ_ρ . Notably the helix properties do not vary when W5 is changed to Y5 in the GWALP23 framework in DLPC.

In DOPC bilayers, semistatic calculations performed using six ²H quadrupolar splittings yield apparent tilt angles of about 6° for both Y⁵GWALP23 and GWALP23 (Table 5). The overall trends are similar for both peptides, with the apparent tilt angles being smaller in DOPC than in DMPC. The direction of tilt ρ_0 increases marginally and in parallel by about 5° from DLPC to DMPC and by about 10° from DMPC to DOPC (Table 5), for both GWALP23 and Y⁵GWALP23. Notably, therefore, the rotation of Y⁵GWALP23 about its helix axis, ranging from about 295° in DLPC to 311° in DOPC, relative to the reference C α of G1,¹¹ is approximately a constant 10° less than that of GWALP23 in each lipid. The Tyr- and Trp-anchored peptide Y⁵GWALP23, indeed, is found to behave very similarly to the original GWALP23 in possessing an adjustable tilt that is sensitive to the lipid membrane thickness. Figures 6A and 7A illustrate the rather similar ρ_0 values for Y⁵GWALP23 in bilayers of different thickness, along with the τ_0 values that increase as the bilayer becomes thinner.

Increased Dynamics for Y^{4,5}GWALP23. When a second tyrosine residue is introduced, in addition to the single Trp near the C-terminus, Y^{4,5}GWALP23 is found to behave quite differently from GWALP23 and Y⁵GWALP23, as indicated first of all by the smaller range of observed ²H quadrupolar splittings (Figure 2). On the basis of precedents with WALP23, and with the related peptide acetyl-GWALW(LA)₆LWLAWA-

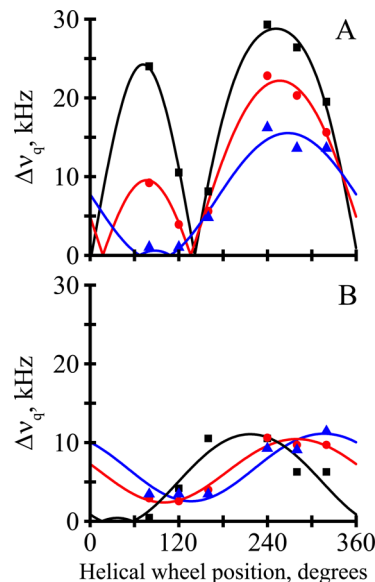


Figure 6. GALA semistatic analysis of Ala-*d*₄ quadrupolar splittings using variable S_{zz} (see ref 11). Quadrupolar wave plots are shown for Y⁵GWALP23 (A) and Y^{4,5}GWALP23 (B) in oriented bilayers of DLPC (black squares), DMPC (red circles), and DOPC (blue triangles). Fitted curves represent theoretical $\Delta\nu_q$ values for orientations corresponding to best-fit values of τ_0 and ρ_0 .

[ethanol]amide (WWALP23), the rather narrow range of ²H quadrupolar splittings strongly suggests increased motional averaging of the ²H signals.^{14,27,39,40} Both the semistatic fit (with S_{zz} of 0.66) and the Gaussian fit (with σ_τ of 27°) indicate a regime of high dynamics for Y^{4,5}GWALP23 in DLPC (Table 4). In the other lipids, consistently low apparent τ_0 values, together with apparent ρ_0 values that diverge from bilayer to

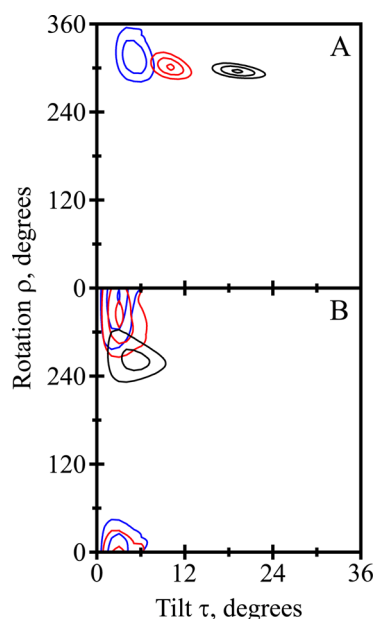


Figure 7. Rmsd contour plots for apparent average tilt τ_0 and rotation ρ_0 resulting from semistatic GALA analysis of Y^5 GWALP23 (A) and $Y^{4,5}$ GWALP23 (B) in DLPC (black), DMPC (red), and DOPC (blue). Contour levels are drawn at 1, 2, and 3 kHz.

bilayer (Figures 6B and 7B; Table 5), again suggest highly dynamic behavior. Indeed, the trends for $Y^{4,5}$ GWALP23 mirror those that have been observed previously for WALP23³¹ and WWALP23.¹⁴ Also, WALP19 is seen to be highly dynamic (large σ_ρ value) in DLPC,⁴¹ although a model-dependent analysis (in which σ_τ is set to zero) suggests that low values of σ_ρ may be allowed under conditions of negative mismatch.⁴¹

Opening the Fluorescence Window. An added advantage of Y^5 GWALP23 is the presence of only a single Trp residue, whose emission λ_{\max} should be unambiguously sensitive to the polarity of the environment of the single indole ring.⁴² It is within this context important to confirm that the fluorescence emission from Y^5 GWALP23 is characteristic of interfacial tryptophan. Indeed, when Y^5 GWALP23 and $Y^{4,5}$ GWALP23 are excited at 295 nm, so as to minimize the contributions from the tyrosines, their emission spectra closely overlap that of GWALP23 (Figure 8), with λ_{\max} being about 335 nm for each peptide. The results suggest similar interfacial locations for the Trp residue(s) in all three peptides. When the excitation wavelength is 280 nm, contributions from the Tyr

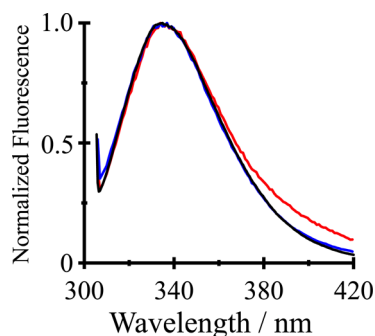


Figure 8. Steady-state fluorescence spectra of GWALP23 (black), Y^5 GWALP23 (blue), and $Y^{4,5}$ GWALP23 (red) in DLPC vesicles excited at 295 nm.

residue(s) are evident (Figure S6 of the Supporting Information). (The Tyr fluorescence emission [at 306 nm], unlike the case of Trp, is not dependent on environment polarity.) The spectra in Figure 8 moreover suggest that fluorescence from Y^5 GWALP23, excited at 295 nm, can serve as an effective probe for potential helix (center-of-mass) translation with respect to the bilayer midplane under the influence of guest residues. For example, when a guest arginine is introduced at position 14 in GWALP23, such a helix translation by about 3 Å has been predicted by coarse-grained molecular dynamics simulations⁴³ but has not yet been observed experimentally.

DISCUSSION

How many Trp residues are needed to maintain a defined orientation, with moderate to low dynamics, and minimal aggregation, for a transmembrane helical domain relative to an interface between water and the interior of a lipid bilayer membrane? Gramicidin channels have eight tryptophans,⁷ while the original WALP peptides employ only four tryptophans.⁸ With the introduction of GWALP23,¹³ we found that as few as two Trp residues can define a preferred orientation for a transmembrane α -helix.¹⁴ Now with the replacement of W5 by Y5, we learn that one interfacial Trp and one interfacial Tyr can confer a stable transmembrane orientation for Y^5 GWALP23. Remarkably, the extent of dynamic averaging of the NMR resonances is *less* when only two Trps—or one Trp and one Tyr—are present than when more than two interfacial aromatic residues are present. In particular, the dynamic averaging is very extensive and involves especially large values of σ_ρ , when four Trps (WALP23 and WWALP23¹⁴) or one Trp with two Tyr ($Y^{4,5}$ GWALP23; this work) provide the interfacial anchoring. Aspects of the data analysis and of the consequences of tyrosine substitutions for the orientation and dynamics of GWALP23 will be discussed in turn.

Agreement of Independent Solid-State NMR Methods. We took advantage of the combined and simultaneous analysis of ^2H quadrupolar splittings, ^{15}N chemical shifts, and $^{15}\text{N}/^1\text{H}$ dipolar couplings for Y^5 GWALP23 in DMPC. The combined goodness-of-fit is essentially the same for GWALP23 and Y^5 GWALP23, giving rmsd values of about 1.2 kHz when 16 observables are analyzed for either of the peptides in DMPC (Table 4). With smaller data sets involving only a single type of parameter, the apparent rmsd values are somewhat lower, typically near 0.6 kHz; yet the deduced values of τ_0 and ρ_0 are essentially the same. For example, semistatic analysis gives a (τ_0 , ρ_0) estimate of (10° , 300°) when the six ^2H $\Delta\nu_q$ values are analyzed alone (Table 5), compared to (16° , 306°) for the set of five ^{15}N chemical shifts and five $^{15}\text{N}/^1\text{H}$ dipolar couplings, or (12° , 298°) when all 16 data points are employed (Table 4). As noted previously,¹³ the independent solid-state NMR methods agree rather well.

Similar Behavior Is Observed for GWALP23 and Its W5 → Y5 Analogue. GWALP23 and Y^5 GWALP23 show similar orientations and dynamics in DLPC, DMPC, and DOPC bilayer membranes (Tables 4 and 5). Remarkably, either a single tyrosine or a single tryptophan at position 5 is sufficient to define the orientation of the N-terminal of the transmembrane peptide with respect to W19 as the sole anchor for the C-terminus. For both peptides in DMPC, the Gaussian dynamic fits show small values of σ_τ (5° – 10°) and moderate values of σ_ρ (65° – 70°) (Table 4). Indeed, if one compares in detail the fits to the Gaussian dynamics in DMPC (Figure 9),

the similar narrow distributions of τ , and broad distributions of ρ , for the two peptides can be directly observed. Notably, the

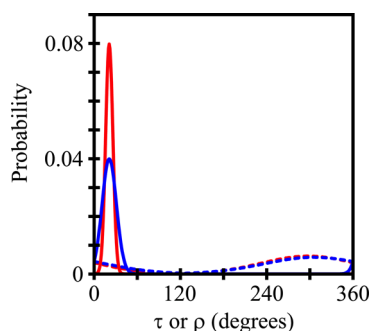


Figure 9. Curves to indicate the widths of the τ distributions (solid curves) and ρ distributions (dashed curves) for GWALP23 (red) and Y⁵GWALP23 (blue), based on Gaussian dynamics analysis of combined GALA and SAMPI4 measurements for each peptide in DMPC.

most probable τ_0 is identical for the two peptides (Figure 9), while the width of the τ distribution increases marginally when Y5 is present, leading to the small increase in σ_τ from $\sim 5^\circ$ to $\sim 10^\circ$ for Y⁵GWALP23 (Table 4). We performed Gaussian analysis also for the peptides in DLPC, using the ^2H NMR data (Table 4). Once again, the results for Y⁵GWALP23 agree with those for GWALP23 itself. In DLPC, the Gaussian and semistatic analyses return nearly equivalent values of τ_0 , in the range of 19° – 23° for both peptides, and the $\sim 10^\circ$ offset in ρ_0 is maintained between W5 and Y5. The Gaussian analyses indicate moderate values of about 30° for σ_ρ and about 15° for σ_τ for GWALP23 and Y⁵GWALP23 in DLPC (Table 4). Importantly, apart from the 10° change in ρ_0 , the Gaussian distributions remain essentially the same when the identity of residue five is modified from Trp to Tyr.

The semistatic fits to the ^2H NMR data reveal similar apparent tilt angles for the W5 and Y5 peptides in DOPC, as well as in DMPC and DLPC (Table 5). In all three lipids, the main effect of Y5 is to alter the most probable direction of the peptide tilt ρ_0 by about 10° (Tables 4 and 5), a result which is independent of whether a semistatic or Gaussian analysis is used to estimate the dynamics. GWALP23 and Y⁵GWALP23 exhibit, furthermore, less extensive motional averaging of their ^2H and ^{15}N resonances than WALP23³⁰ or WWALP23¹⁴ in each of the lipid membranes. With this direct comparison of residues W5 and Y5 in GWALP23 now available, it would be of future interest to compare also the substitution of W19 with Y19.

Enhanced Dynamics When Y4 Is Introduced into Y⁵GWALP23. To address the question of whether one or two Tyr residues would be preferable for defining a transmembrane helix orientation, we compared the properties of the Y5 and Y4,5 peptides. The comparison (Figures 6 and 7) indicates a loss of systematic behavior when Y4 is introduced alongside Y5. With Y4 present, the observed ^2H $\Delta\nu_q$ magnitudes span only a small range in each lipid, ρ_0 becomes unpredictable in membranes of different thickness, and τ_0 no longer scales with the bilayer thickness. Indeed, the dynamic properties of Y^{4,5}GWALP23, as revealed by ^2H NMR, resemble those of WALP19,^{11,12} WALP23,^{30,31,39,40,44,45} and W^{2,22}W^{5,19}ALP23,¹⁴ all of which possess four Trp residues. It is nevertheless conceivable that also the loss of the hydrophobic L4 residue

itself could contribute to the apparent changes in the peptide dynamics, a situation which could be checked by investigating the properties of the single-tyrosine mutant Y⁴GWALP23 peptide. Regardless of such a possibility, the present results suggest that “extra” aromatic residues may compete with each other at the membrane interface.

Summarizing Perspective: Implications for the Number of Interfacial Aromatic Residues. The accumulated results to date indicate, concerning the preferred number of aromatic Trp or Tyr residues to anchor each end of a transmembrane helix, that “one is enough” and “two are too many”. When (W⁵)GWALP23 and Y⁵GWALP23 are compared, the orientations and dynamic properties are found to be remarkably similar in three different lipid bilayer membranes; namely, Tyr is found to define a preferred peptide orientation as effectively as Trp (at the N-terminal). (The relative anchoring potential of Tyr versus Trp has yet to be established at the C-terminal.) Importantly, including additional aromatic residues—whether one more tyrosine in Y^{4,5}GWALP23, or two more tryptophans (for example, in WALP23 or WWALP23)—markedly increases the extent of the peptide dynamics. It is plausible that the increased dynamic behavior may be due to competition among different aromatic residues for preferred positions with respect to the head groups of the lipid bilayer.

■ ASSOCIATED CONTENT

📄 Supporting Information

Chromatogram, mass spectra, and additional NMR and fluorescence spectra for characterization of peptides and lipids. This material is available free of charge via the Internet at <http://pubs.acs.org>.

■ AUTHOR INFORMATION

Corresponding Author

*Tel (479) 575-4976; Fax (479) 575-4049; e-mail rk2@uark.edu.

Funding

This work was supported in part by NSF grant MCB 0841227 and by the Arkansas Biosciences Institute. The peptide facility is supported by NIH grants RR31154 and RR16460. The NMR facilities are supported by NIH grant RR31154 and the Biotechnology Research Center for NMR Molecular Imaging of Proteins at the University of California, San Diego, which is supported by NIH grant P41EB002031.

Notes

The authors declare no competing financial interest.

■ ACKNOWLEDGMENTS

We thank Marvin Leister for extensive help with the deuterium NMR experiments.

■ ABBREVIATIONS

CD, circular dichroism; DLPC, 1,2-dilauroylphosphatidylcholine; DMPC, 1,2-dimyristoylphosphatidylcholine; DOPC, 1,2-dioleoylphosphatidylcholine; DMPC-ether, 1,2-di-*O*-myristoylphosphatidylcholine; DHPC-ether, 1,2-di-*O*-hexylphosphatidylcholine; Fmoc, fluorenylmethoxycarbonyl; GALA, geometric analysis of labeled alanines; GWALP23, acetyl-GGALW-(LA)₆LWLAGA-[ethanol]amide; MtBE, methyl-*tert*-butyl ether; PISEMA, polarization inversion spin exchange at magic angle; rmsd, root-mean-squared deviation; TFA, trifluoroacetic

acid; WWALP23, acetyl-GWALW(LA)₆LWLAWA-[ethanol]-amide.

REFERENCES

- (1) Davis, J. H., Hodges, R. S., and Bloom, M. (1982) The Interaction between a Synthetic Amphiphilic Polypeptide and Lipids. *Biophys. J.* 37, 170–171.
- (2) Davis, J. H., Clare, M. D., Hodges, R. S., and Bloom, M. (1983) The Interaction between a Synthetic Amphiphilic Polypeptide and Lipids in a Bilayer Structure. *Biochemistry* 22, 5298–5305.
- (3) Zhang, Y. P., Lewis, R. N., Henry, G. D., Sykes, B. D., Hodges, R. S., and McElhaney, R. N. (1995) Peptide models of helical hydrophobic transmembrane segments of membrane proteins. I. Studies of the conformation, intrabilayer orientation, and amide hydrogen exchangeability of Ac-K₂-(LA)₁₂-K₂-amide. *Biochemistry* 34, 2348–2361.
- (4) Landolt-Marticorena, C., Williams, K. A., Deber, C. M., and Reithmeier, R. A. (1993) Non-random distribution of amino acids in the transmembrane segments of human type I single span membrane proteins. *J. Mol. Biol.* 229, 602–608.
- (5) Schiffer, M., Chang, C. H., and Stevens, F. J. (1992) The functions of tryptophan residues in membrane proteins. *Protein Eng. S.* 213–214.
- (6) Killian, J. A., Prasad, K. U., Urry, D. W., and de Kruijff, B. (1989) A mismatch between the length of gramicidin and the lipid acyl chains is a prerequisite for H_{II} phase formation in phosphatidylcholine model membranes. *Biochim. Biophys. Acta* 978, 341–345.
- (7) O'Connell, A. M., Koeppe, R. E. II, and Andersen, O. S. (1990) Kinetics of gramicidin channel formation in lipid bilayers: transmembrane monomer association. *Science* 250, 1256–1259.
- (8) Killian, J. A., Salemink, I., de Planque, M. R., Lindblom, G., Koeppe, R. E. II, and Greathouse, D. V. (1996) Induction of nonbilayer structures in diacylphosphatidylcholine model membranes by transmembrane alpha-helical peptides: importance of hydrophobic mismatch and proposed role of tryptophans. *Biochemistry* 35, 1037–1045.
- (9) de Planque, M. R., Kruijter, J. A., Liskamp, R. M., Marsh, D., Greathouse, D. V., Koeppe, R. E. II, de Kruijff, B., and Killian, J. A. (1999) Different membrane anchoring positions of tryptophan and lysine in synthetic transmembrane alpha-helical peptides. *J. Biol. Chem.* 274, 20839–20846.
- (10) de Planque, M. R., Boots, J. W., Rijkers, D. T., Liskamp, R. M., Greathouse, D. V., and Killian, J. A. (2002) The effects of hydrophobic mismatch between phosphatidylcholine bilayers and transmembrane alpha-helical peptides depend on the nature of interfacially exposed aromatic and charged residues. *Biochemistry* 41, 8396–8404.
- (11) van der Wel, P. C., Strandberg, E., Killian, J. A., and Koeppe, R. E. II (2002) Geometry and intrinsic tilt of a tryptophan-anchored transmembrane alpha-helix determined by ²H NMR. *Biophys. J.* 83, 1479–1488.
- (12) Lee, J., and Im, W. (2008) Transmembrane helix tilting: insights from calculating the potential of mean force. *Phys. Rev. Lett.* 100, 018103.
- (13) Vostrikov, V. V., Grant, C. V., Daily, A. E., Opella, S. J., and Koeppe, R. E. II (2008) Comparison of “Polarization inversion with spin exchange at magic angle” and “geometric analysis of labeled alanines” methods for transmembrane helix alignment. *J. Am. Chem. Soc.* 130, 12584–12585.
- (14) Vostrikov, V. V., Daily, A. E., Greathouse, D. V., and Koeppe, R. E. II (2010) Charged or aromatic anchor residue dependence of transmembrane peptide tilt. *J. Biol. Chem.* 285, 31723–31730.
- (15) Marassi, F. M., and Opella, S. J. (2000) A solid-state NMR index of helical membrane protein structure and topology. *J. Magn. Reson.* 144, 150–155.
- (16) Wang, J., Denny, J., Tian, C., Kim, S., Mo, Y., Kovacs, F., Song, Z., Nishimura, K., Gan, Z., Fu, R., Quine, J. R., and Cross, T. A. (2000) Imaging membrane protein helical wheels. *J. Magn. Reson.* 144, 162–167.
- (17) Hall, B. A., Armitage, J. P., and Sansom, M. S. P. (2011) Transmembrane Helix Dynamics of Bacterial Chemoreceptors Supports a Piston Model of Signalling. *PLOS Comput. Biol.* 7, e1002204.
- (18) Kirchberg, K., Kim, T. Y., Moller, M., Skegros, D., Raju, G. D., Granzin, J., Buldt, G., Schlesinger, R., and Alexiev, U. (2011) Conformational dynamics of helix 8 in the GPCR rhodopsin controls arrestin activation in the desensitization process. *Proc. Natl. Acad. Sci. U. S. A.* 108, 18690–18695.
- (19) Thomas, R., Vostrikov, V. V., Greathouse, D. V., and Koeppe, R. E. II (2009) Influence of proline upon the folding and geometry of the WALP19 transmembrane peptide. *Biochemistry* 48, 11883–11891.
- (20) Pace, C. N., Vajdos, F., Fee, L., Grimsley, G., and Gray, T. (1995) How to measure and predict the molar absorption coefficient of a protein. *Protein Sci.* 4, 2411–2423.
- (21) Davis, J. H., Jeffrey, K. R., Bloom, M., Valic, M. I., and Higgs, T. P. (1976) Quadrupolar echo deuteron magnetic resonance spectroscopy in ordered hydrocarbon chains. *Chem. Phys. Lett.* 42, 390–394.
- (22) Wu, C. H., Ramamoorthy, A., and Opella, S. J. (1994) High-Resolution Heteronuclear Dipolar Solid-State NMR Spectroscopy. *J. Magn. Reson.* A 109, 270–272.
- (23) Nevzorov, A. A., and Opella, S. J. (2003) A “magic sandwich” pulse sequence with reduced offset dependence for high-resolution separated local field spectroscopy. *J. Magn. Reson.* 164, 182–186.
- (24) Cook, G. A., and Opella, S. J. (2010) NMR studies of p7 protein from hepatitis C virus. *Eur. Biophys. J.* 39, 1097–104.
- (25) Nevzorov, A. A., and Opella, S. J. (2007) Selective averaging for high-resolution solid-state NMR spectroscopy of aligned samples. *J. Magn. Reson.* 185, 59–70.
- (26) Triba, M. N., Warschawski, D. E., and Devaux, P. F. (2005) Reinvestigation by Phosphorus NMR of Lipid Distribution in Bicelles. *Biophys. J.* 88, 1887–1901.
- (27) Vostrikov, V. V., Grant, C. V., Opella, S. J., and Koeppe, R. E. II (2011) On the Combined Analysis of ²H and ¹⁵N/¹H Solid-State NMR Data for Determination of Transmembrane Peptide Orientation and Dynamics. *Biophys. J.* 101, 2939–2947.
- (28) van der Wel, P. C. A., Reed, N. D., Greathouse, D. V., and Koeppe, R. E. II (2007) Orientation and Motion of Tryptophan Interfacial Anchors in Membrane-Spanning Peptides. *Biochemistry* 46, 7514–7524.
- (29) Gleason, N. J., Vostrikov, V. V., and Koeppe, R. E. (2009) Comparison of Mechanical and Magnetic Alignment of WALP-like Peptides for Solid-State NMR. *Biophys. J. Suppl.* 445a, Abstract 2349-Pos.
- (30) Strandberg, E., Esteban-Martin, S., Salgado, J., and Ulrich, A. S. (2009) Orientation and dynamics of peptides in membranes calculated from ²H-NMR data. *Biophys. J.* 96, 3223–3232.
- (31) Strandberg, E., Ozdirekcan, S., Rijkers, D. T., van der Wel, P. C., Koeppe, R. E. II, Liskamp, R. M., and Killian, J. A. (2004) Tilt angles of transmembrane model peptides in oriented and non-oriented lipid bilayers as determined by ²H solid-state NMR. *Biophys. J.* 86, 3709–3721.
- (32) Nevzorov, A. A., Mesleh, M. F., and Opella, S. J. (2004) Structure determination of aligned samples of membrane proteins by NMR spectroscopy. *Magn. Reson. Chem.* 42, 162–171.
- (33) Saito, H., Ando, I., and Ramamoorthy, A. (2010) Chemical shift tensor - the heart of NMR: Insights into biological aspects of proteins. *Prog. Nucl. Magn. Reson. Spectrosc.* 57, 181–228.
- (34) Bechinger, B., Resende, J. M., and Aisenbrey, C. (2011) The structural and topological analysis of membrane-associated polypeptides by oriented solid-state NMR spectroscopy: established concepts and novel developments. *Biophys. Chem.* 153, 115–125.
- (35) Ketchum, R. R., Lee, K. C., Huo, S., and Cross, T. A. (1996) Macromolecular structural elucidation with solid-state NMR-derived orientational constraints. *J. Biomol. NMR* 8, 1–14.
- (36) Tian, C., Gao, P. F., Pinto, L. H., Lamb, R. A., and Cross, T. A. (2003) Initial structural and dynamic characterization of the M2 protein transmembrane and amphipathic helices in lipid bilayers. *Protein Sci.* 12, 2597–2605.

- (37) Vostrikov, V. V. Ph.D. Dissertation, University of Arkansas, 2011.
- (38) Killian, J. A., Taylor, M. J., and Koeppe, R. E. II (1992) Orientation of the valine-1 side chain of the gramicidin transmembrane channel and implications for channel functioning. A ^2H NMR study. *Biochemistry* 31, 11283–11290.
- (39) Ozdirekcan, S., Etchebest, C., Killian, J. A., and Fuchs, P. F. (2007) On the orientation of a designed transmembrane peptide: toward the right tilt angle? *J. Am. Chem. Soc.* 129, 15174–15181.
- (40) Esteban-Martin, S., and Salgado, J. (2007) The dynamic orientation of membrane-bound peptides: bridging simulations and experiments. *Biophys. J.* 93, 4278–4288.
- (41) Strandberg, E., Esteban-Martin, S., Ulrich, A. S., and Salgado, J. (2012) Hydrophobic mismatch of mobile transmembrane helices: Merging theory and experiments. *Biochim. Biophys. Acta*, DOI: 10.1016/j.bbamem.2012.01.023.
- (42) Ren, J., Lew, S., Wang, Z., and London, E. (1997) Transmembrane orientation of hydrophobic α -helices is regulated both by the relationship of helix length to bilayer thickness and by the cholesterol concentration. *Biochemistry* 36, 10213–10220.
- (43) Vostrikov, V. V., Hall, B. A., Greathouse, D. V., Koeppe, R. E. II, and Sansom, M. S. P. (2010) Changes in Transmembrane Helix Alignment by Arginine Residues Revealed by Solid-State NMR Experiments and Coarse-Grained MD Simulations. *J. Am. Chem. Soc.* 132, 5803–5811.
- (44) Monticelli, L., Tieleman, D. P., and Fuchs, P. F. (2010) Interpretation of ^2H -NMR experiments on the orientation of the transmembrane helix WALP23 by computer simulations. *Biophys. J.* 99, 1455–1464.
- (45) Holt, A., Rougier, L., Reat, V., Jolibois, F., Saurel, O., Czaplicki, J., Killian, J. A., and Milon, A. (2010) Order parameters of a transmembrane helix in a fluid bilayer: case study of a WALP peptide. *Biophys. J.* 98, 1864–1872.
- (46) DeLano, W. L. (2002) *The PyMOL Molecular Graphics System*.
- (47) Pulay, P., Scherer, E. M., van der Wel, P. C., and Koeppe, R. E. II (2005) Importance of tensor asymmetry for the analysis of ^2H NMR spectra from deuterated aromatic rings. *J. Am. Chem. Soc.* 127, 17488–17493.